Parametric Study and Optimization of Ceiling Fan Blades for Improved Aerodynamic Performance

E. Adeeb[1], A. Maqsood[2†], A. Musthaq[2] and C. H. Sohn[1]

[1] Kyungpook National University, Daegu, 702-701, South Korea
[2] Research Centre for Modeling & Simulation, National University of Sciences and Technology, Islamabad, 44000, Islamic Republic of Pakistan

†*Corresponding Author Email: adnan@rcms.nust.edu.pk*

ABSTARCT

This paper includes parametric study and optimization of non-linear ceiling fan blades by combining the techniques of Design of Experiments (DOE), Response Surface Methods (RSM) and Computational Fluid Dynamics (CFD). Specifically, the nonlinear (elliptical) planform shape of ceiling fan blade is investigated in conjunction with blade tip width, root and tip angle of attack. Sixteen cases are designed for three blade ceiling fan using two level full factorial model. The flow field is modeled using Reynolds-Averaged-Navier-Stokes approach. The performance variables used to formulate a multi-objective optimization problem are volumetric flow rate, torque and energy efficiency. Response Surface Method is used to generate the optimized design for non-linear ceiling fan blade profile. The results reveal that the interactions between the design variables play a significant role in determining the performance. It is concluded that the nonlinear forward sweep has a moderate effect on response parameters.

Keywords: Design of experiments; Performance engineering; Blade design; Computational fluid dynamics; Response surface methods; Nonlinear blade profile.

NOMENCLATURE

A	forward Sweep	τ	stress tensor
B	root angle of attack	V	velocity field
C	tip angle of attack	∇	operator
C_b	constant	u	velocity component
D	tip width	Yv	destruction of turbulent viscosity
F	external body force	$\bar{u}$	time averaged velocity component
G	production of turbulent viscosity	u'	fluctuating velocity
p	static pressure	u'_j	instantaneous velocity component
S	source term	β	coefficient of regression
ν	kinematic viscosity	ρ	density of the fluid
X	coefficient of repressor	τ_{ij}	Reynolds stress tensor
Y	response of the system	δ_{ij}	Kronecker delta

1. INTRODUCTION

Ceiling fans are widely used by inhabitants of tropical regions for indoor comfort. Sathaye and Phadke *et al.* (2012) conducted cost-benefit analysis to establish the need of developing energy efficient ceiling fan technology for India, China and US.

The energy efficiency is conceptualized in terms of less power consumption and associated carbon emissions. The study indicated that integration of existing commercially viable technologies can improve the energy efficiency of ceiling fans by fifty percent. If ceiling fan centric technologies are developed by 2020, this will translate into power savings of 70 Tera Watt Hours per Year. The associated reduction of carbon dioxide emissions will be 25 million metric tons per year. Scholarly efforts are required for design, development and integration of energy-efficient ceiling fan technology. A great deal of interest has already

emerged during the last several years for energy efficient ceiling fans. Bladeless fan studies of Jafari and Afshin *et al.* (2015) are one such example that have attracted attention of technology protagonists.

Ankur and Rochan *et al.* (2004) experimentally investigated the flow field of a ceiling fan. Smoke visualization and vane anemometers were used for visualization and flow velocity measurements respectively. The maximum recorded velocity is between 2 and 3 m/s below the ceiling fan disk. Feasibility about using winglets at blade-tips was also assessed. Parker and Challahan *et al.* (2000) made an effort to find a design which had maximum air flow, uniform air movement and minimum acoustic signature in the room. Out of three different designs considered, tapered blades performed best. Experimental studies by Chiang and Pan *et al.* (2007) , Falahat (2011) and Bhortake and Lachure *et al.* (2014) have focused on improving aerodynamic performance of ceiling fan, by carrying out blade design refinement. Bhortake and Lachure *et al.* (2014) used Response Surface Methodology (RSM) and generated design space with three fan blades, three down rod lengths, three room sizes and three fan rotation speeds. Falahat (2011) found optimal revolutions and angle of attack of a flat blade ceiling fan in a room. The effect of number of blades on aerodynamic efficiency was also investigated. The results concluded that a fan with four blades based on a specific design results in maximum air circulation in the room. The flow behaviour for a fan did not change excessively with four, five and six blades. The only penalization with the increase in number of blades was on energy consumption.

Parker and Challahan *et al.* (2000) reported that ceiling fans used in combination with higher thermostat of air-conditioning results in significant energy consumption savings. Schiavon and Melikov (2008) investigates cooling effects with improved air circulation and report reduction in electricity from 10 to 28 percent. Schmdit and Patterson (2001) studied high efficiency tropical ceiling fan and a conventional fan. A comparative study is done between approximate volume flow rate, mechanical power and electrical input power on the shaft. The new design saves electricity almost by a factor of two. Azim (2014) developed a mathematical expression for axial velocity distribution of a ceiling fan. This mathematical formulation is in good agreement with computational and mathematical data of velocity field of ceiling fans. Ramadan and Nadar (2011) derived a mathematical formula which is helpful to find the velocity of the fan above the ground floor in a defined space. The study reports that maximum tangential velocity is at the blade tip and it decreases as the air moves downward. Moreover, the tangential velocity increases with an influence of four if the fan speed is increased with the same influence. Lin and Hsieh (2014) predict and pinpoint the flow pattern, airflow rate, efficiency, and noise for ceiling fans with different design parameters using numerical and experimental techniques. The study reports that for an inadequate housing, 'inhale-return' phenomenon can occur that affects the performance and power consumption of a ceiling fan because its inlet and outlet are almost located at the same plane. Afaq and Maqsood *et al.* (2014) , Adeeb and Maqsood *et al.* (2015) and Adeeb and Maqsood *et al.* (2015) have done blade parametric studies and investigated the effect of number of blades on ceiling fan performance respectively. Results of improvement in air delivery, mass flow rate and service value of Commercial Off The Shelf (COTS) ceiling fans by modifying blade geometry are reported. The parameters considered for design improvement are rake angles, root and tip bent angles and positions. Aziz and Shahat *et al.* (2012) experimentally and numerically investigated the behaviour of ceiling fan induced flow field inside a ventilated room and observed the effects of vortices, round and square ceiling diffuser on thermal comfort. Results show that energy saved by square or round diffuser is 1.5 times greater than vortex diffuser.

Rizk and El-Deberky *et al.* (2015) studied computationally and mathematically effect of ceiling and wall on air temperature during night in extremely hot climates. During night, indoor temperature of the building is high due to gain of heat and the indoor temperature is going beyond thermal comfort. Nawaz and Kanti *et al.* (2012) established a fuzzy inference system that controls Revolutions Per Minute (rpm) of ceiling fan according to temperature of environment and relative humidity. For validation, experimental data is compared with different mathematical procedures. Using fuzzy logic toolbox they developed a simulation scheme to investigate the result. Amano and Lee *et al.* (2005) studied experimental and CFD/FEA simulation of large axial fan effect on flow. The flow pattern is changed by adding a radiator in front of axial fan. However, it produces around 10 to 20 percent stresses on the blade surface. Ho and Rosario *et al.* (2005) made an effort to find the best thermal comfort level with the combination of air-conditioners and ceiling fans. A two dimensional steady state problem was solved using CFD simulation. Fourteen different simulation cases were run for different locations of inlet diffuser and the position of the fan. Momoi and Sagara *et al.* (2004) studied the velocity profile of a ceiling fan in an air-conditioned room. CFD results show greater value of velocity profile near the rotational centre of the ceiling fan. Lin and Hsieh *et al.* (2013) developed a new approach for installation of ceiling fans that have an enclosed housing and is hidden inside the ceiling floor. Using experimental and numerical methodology, the flow behaviour is predicted with different operating conditions and geometric housing. Conclusions revealed that as air moves towards the floor, different flow patterns are generated and demonstrate "inhale-return" phenomenon only when housing comprises of anomalous shaped high ring-plate and outlet-inlet ratio. Prabhakaran and Kumar (2012) experimentally compared the composite materials fan blades with aluminium fan blades. Results show that composite blade save 34% fabrication cost and 30% power because of 28% weight reduction.

Lubliner and Douglass *et al.* (2004) made an effort to make a solar powered ceiling fan which is cost

effective and environment friendly. A comparative study is done between three and four blade ceiling fan and the results show little difference between velocity profile and RPM. Four blade ceiling fan should be used for better air circulation and three blades for energy efficiency. Idahosa and Golubev *et al.* (2008) focused on Multi-disciplinary Design Optimization (MDO) to make an optimized design of a fan blade using CFD. Three prototypes of fan models achieved 11%, 13.85% and 11.61% respectively.

Researchers round the globe have studied and optimized linear profiles of ceiling fans. In this research endeavour, the nonlinear (elliptical) plan form shape of blade is studied in conjunction with blade tip width, root and tip angle of attack. The flow field is studied and the fan surface is modelled using Reynolds-Averaged-Navier-Stokes approach. By applying Design of Experiments (DOE), 16 experiments are designed for three blade ceiling fan using 2^k factorial model. A multi-objective optimization problem is formulated with three performance variables; volumetric flow rate, torque and energy efficiency. Comparisons between these 16 blades are done by using Response Surface Method (RSM) and subsequently an optimized design is proposed. The research reveals that the interactions between the design variables play a significant role in determining the performance. The tip angle of attack is found to be most important and influential. Moreover, the nonlinear forward sweep has a moderate effect on response parameters.

2. PROBLEM FORMULATION AND METHODS

A ceiling fan consists of a hub, electric motor, blades and the whole assembly is mounted to the ceiling of the room. The main purpose of the hub is to house the electric motor and hold the blades at specific angles.

An electric motor converts electrical energy to mechanical energy and spin the blades at desired rpm. A 56″ (1.4224 m) diameter commercially available fan is used as a benchmark design in this study (Fig. 1). The diameter is based on the calculated circular area swept by the ceiling fan during operation. Ceiling fan blades are made of aluminum with a thickness of about 0.001 m, spans 0.568 m and three blades are 120 degree apart from one another. The part of the blade which is attached to the hub is called root while the other is tip. The blade part which makes first contact with air is called leading edge and other part after which air rejoins is referred as trailing edge.
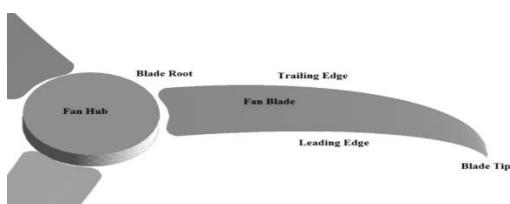

Fig. 1. Ceiling fan geometry.

2.1. Experimental Setup and Data Collection

Experiments are conducted in a test facility consisting of a square wooden room with dimension of 6.5 m in length and width and 3.5 m height. Ceiling fan is installed in a duct 1 m below the ceiling whose diameter is 1.56 m. Fan height from the ground is 2.5 m. A tachometer is also hanged in the duct to measure the rotational motion in Revolutions Per Minute (rpm). Entire controlling instruments and multi-meter are installed on the wall. Electronic instruments showed readings in real time. Duct and controlling instruments are shown in Fig. 2. Air velocity is measured diagonally on the four sides of the room from hub to tip towards the wall with vane anemometer.
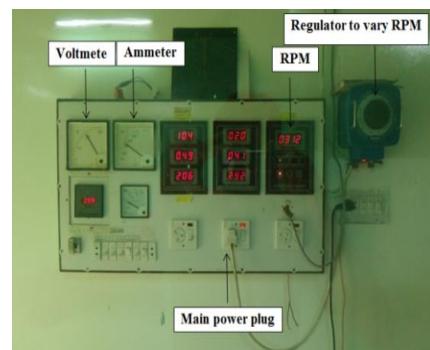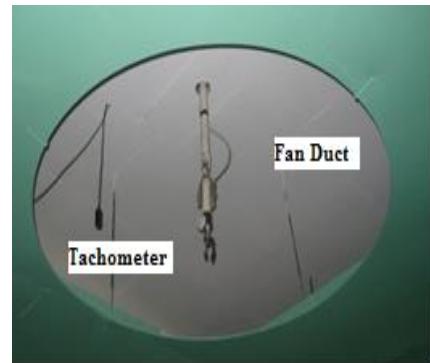

Fig. 2. Testing duct, tachometer, display panel and anemometer of testing lab.

For each reading vane anemometer is placed for two minutes on the desired position before capturing the maximum velocity. The ceiling fan is switched for two hours before starting the experiment so the flow can be fully developed in the testing facility.

Vane anemometer took fourteen readings in each direction (A, AA, B & BB). Further calculations are done by taking the average of these points. All points are calculated 1.5 m below the ceiling fan. The first point is at position 0.03 m and all other points are 0.06 m apart from each other. Air velocity for experimental case is tabulated in Table 1.

Table 1 Experimentally measured air velocity

Reading Number	Distance Hub to Tip (m)	Air Velocity (m/s)				Mean
		A	AA	B	BB	
1	0.03	2.03	2.29	2.45	2.33	2.27
2	0.09	2.52	2.64	2.42	2.32	2.47
3	0.15	2.51	2.72	2.68	2.68	2.64
4	0.21	2.52	2.56	2.56	2.61	2.56
5	0.27	2.7	2.69	2.77	2.67	2.7
6	0.33	2.84	2.8	2.68	2.83	2.78
7	0.39	2.74	2.77	2.64	2.81	2.74
8	0.45	2.64	2.76	2.39	2.8	2.64
9	0.51	2.23	2.53	1.8	2.57	2.28
10	0.57	1.92	2.34	1.46	2.39	2.02
11	0.63	1.53	1.97	1	1.94	1.61
12	0.69	0.89	1.83	0.93	1.26	1.22
13	0.75	0.43	0.75	0.77	0.77	0.68
14	0.81	0	0.32	0.67	0.38	0.34

2.2. Mathematical Formulation

Fluid motion is governed by conservation laws. The conservation law states that if there is no source or sink then net flux across the surface bounding in a controlled volume is zero. There are three governing equations of fluid mechanics which are momentum, continuity and energy equations. Since the flow is of incompressible nature, energy equation is not considered. The continuity equation can be expressed as:

$$\frac{\partial \rho}{\partial t} + \nabla . (\rho \boldsymbol{V}) = 0 \qquad (1)$$

The first term in Eq. (1) is the rate of change of density (mass per unit volume). The second term describes the net flow of mass out of the element across its boundaries and is called the convective term.

$$\frac{\partial \rho}{\partial t} + \frac{\partial (\rho u)}{\partial x} + \frac{\partial (\rho v)}{\partial y} + \frac{\partial (\rho w)}{\partial z} = 0 \qquad (2)$$

Since, density ρ is constant for an incompressible fluid,

$$\frac{\partial u}{\partial x} + \frac{\partial v}{\partial y} + \frac{\partial w}{\partial z} = 0 \Rightarrow \nabla . \boldsymbol{V} = 0 \qquad (3)$$

Eq. (3) is a general form of the continuity equation for incompressible flows. By using continuity and momentum equations, Claude-Louis Navier and George Gabriel Stokes in 1822 developed Navier-Stokes equations. Navier-Stokes equations can be used to determine the velocity vector field that

applies to a fluid, by some given initial conditions. The general form of the Navier - Stokes equation can be seen in Eq. (4). This equation states that force is composed of three components: pressure, stress and body force term

$$\rho \frac{DV}{Dt} = -\nabla p + \nabla . \tau + f \qquad (4)$$

where ρ is the density of the fluid, τ is stress tensor, V is the velocity of the flow, p is the pressure, f represents the body force and ∇ is the differential operator.

$$\rho \left(\frac{\partial V}{\partial t} + (V . \nabla)V \right) = -\nabla p + \nabla . \tau + f \qquad (5)$$

$$\frac{\partial (\rho u_i)}{\partial t} + \frac{\partial (\rho u_i u_j)}{\partial x_j}$$
$$= -\frac{\partial p}{\partial x_i} + \frac{\partial \tau_{ij}}{\partial x_j} + \rho g_i$$
$$+ F_i \qquad (6)$$

$$\tau_{ij} = \left[\mu \left(\frac{\partial u_i}{\partial x_j} + \frac{\partial u_j}{\partial x_i} \right) \right] - \frac{2}{3} \mu \frac{\partial u_i}{\partial x_i} \delta_{ij} \qquad (7)$$

where τ_{ij} is the Reynolds stress tensor, p is the static pressure, F_i is external body force in the ith direction, δ_{ij} is the Kronecker delta and is equal to unity when $i=j$; and zero when $i \neq j$ and g_i is gravitational acceleration in i^{th} direction.

2.3. Geometry Generation for Nonlinear Ceiling Fan Blade Profile

The mathematical formulation of non-linear ceiling fan blade is defined using parametric equation of ellipse in Eq. (8).

$$x = a \, Cos\,(t) \quad y = b \, Sin\,(t) \qquad (8)$$

$$\begin{bmatrix} 1 & 0 & 0 \\ 0 & Cos(t) & -Sin(t) \\ 0 & Sin(t) & Cos(t) \end{bmatrix} \qquad (9)$$

where $0 \leq t \leq 2\pi$. In blade generation semi major axis represents the length and semi minor axis represents non-linear sweep in the blade. Firstly, its different parameters are identified like length of the blade (*a*) width, non-linearity in the ceiling fan blade (*b*) and parameter *t* of elliptical equation. The geometric profiles are modeled in Matlab®. Values of angle of attack from tip to root are assigned and then each coordinate multiplied by a rotation matrix to rotate the blade in x- direction rotation matrix shown in Eq. (9). Then, the average of the upper and lower blade is calculated and subtracted from *z* coordinate of the blade. The same is done for root and tip coordinates. Finally these coordinates of ceiling fan blades are exported in Gambit® where all final geometries are pre-processed for further analysis.

2.4. Computational Setup

In recent years, CFD techniques have been extensively applied to many engineering applications because it saves experimental efforts and time. Several applied issues of predicting air flow patterns, such as from Maqsood and Masud *et al.* (2007), Tripathi and Moulic (2012), Singh and

Garg *et al.* (2013) and Sivakumar and Surendhar *et al.* (2015) are addressed using CFD techniques. In this study, finite volume based CFD software Ansys Fluent® is used. The computational model consists of two domains; stationary (Room) and rotating (Fan Disk) both domains are connected by frozen rotor interface. The steady state incompressible flow Reynolds-Averaged-Navier-Stokes (RANS) system of equations is solved using coupled-implicit formulation. The Reynolds − Averaged − Navier - Stokes equation in general can be seen in Eq. (10).

$$\frac{\partial(\rho u_i)}{\partial t} + \frac{\partial(\rho u_i u_j)}{\partial x_j}$$
$$= -\frac{\partial p}{\partial x_i} + \frac{\partial \tau_{ij}}{\partial x_j} + \frac{\partial\left(-\rho \overline{u_i' u_j'}\right)}{\partial x_j}$$
$$+ F_x \tag{10}$$

where u_j' is the instantaneous velocity component *(i = 1,2, 3)*. Viscous effects in flow are captured by using turbulence modeling. Adiabatic wall boundary condition and no-slip velocity is imposed at room walls and at the surface of the blades. For simulating the system, 300 rpm is specified for rotating domain, total temperature value is 288K and total pressure of 101325 Pa is used. All calculations are done with 0.7 million meshed cells and 1 million meshed cells on room and ceiling fan respectively. Computations are executed on HP core i-7 with 16 GB of RAM. For meshing unstructured tetrahedral mesh elements are used to mesh stationary and rotating domain as shown in Fig. 3. Before deciding mesh size, grid independence study is carried out for both domains. The purpose of this study is to assure that there is no effect on results by changing mesh size. Three different mesh sizes are used for grid independence study. The grid with best results in terms of flow profile and computational efficiency is then selected for further analysis of air flow rate.
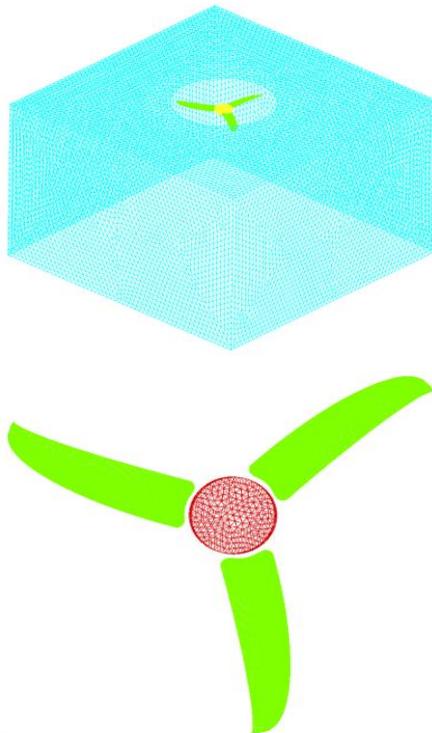

Fig. 3. Unstructured room mesh and surface mesh on fan blades and hub.

2.5. Validation Studies

For grid independence study of room three meshes are made coarse, medium and fine with a number of cells 0.7, 0.9 and 1.1 million respectively. These meshes are created in Gambit® and simulated in Fluent® solver. Results of all simulations are extracted in Tecplot360® for understanding the flow physics. Fig. 4 shows that all mesh qualities are above 95% agreement with each other. So, for room the mesh with 0.7 million cells is chosen as a baseline grid size for further simulation because it saves computational time and gives accurate result.
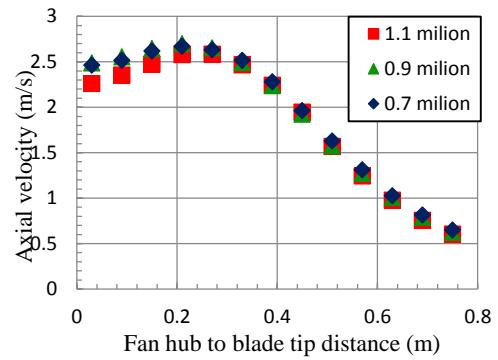

Fig. 4. Grid independence study for room.

Now for ceiling fan disk, three meshes are created with coarse (0.8 million), medium (1 million) and fine (1.3 million) mesh cells. The graph between these three mesh sizes, is shown in Fig. 5. The mesh with 1 million mesh cells is chosen for further simulation because it gave accurate results. The choice of medium mesh quality is done because we want to capture the flow attributes accurately on ceiling fan blade.
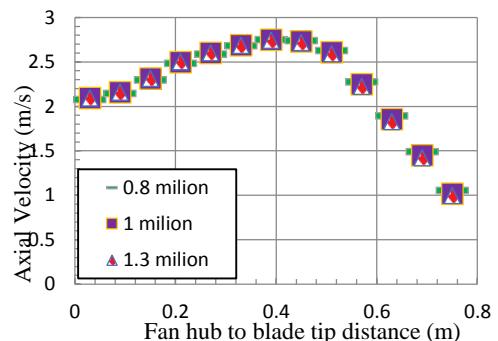

Fig. 5. Grid independence study for fan disk.

Three different turbulence models $k - \epsilon$, $k - \omega$ and Spalart-Allmaras were studied with 0.7 million meshed cells on room and 1 million meshed cells for a ceiling fan for capturing the viscous effects correctly. A comparison of turbulence models is shown in Fig. 6. All the models show similar behavior of velocity magnitudes. The graph is plotted between fan hub towards blade tip distance and axial velocity. The numerical results with Spalart (1992) turbulence model are found to be in good agreement with experimental data. SA model is a one equation model designed especially for wall-

Table 2 Geometric parameters, range and response parameters

Serial Number	Geometric Parameters with Symbol	Selected Parameters		Response Parameters		
		Low	High			
1	Forward Swept (A)	0.05 m	0.15 m			
2	Root Angle of Attack (B)	6 deg	12 deg	Volumetric Flow Rate	Torque	Energy Efficiency
3	Tip Angle of Attack (C)	6 deg	12 deg			
4	Tip Width (D)	0.058 m	0.117m			

Table 3 Geometric designs with associated levels

Design Number	Forward Swept (A)	Root AOA (B)	Tip AOA (C)	Tip Width (D)
1	0.05	6	6	0.058
2	0.15	6	6	0.058
3	0.05	12	6	0.058
4	0.15	12	6	0.058
5	0.05	6	12	0.058
6	0.15	6	12	0.058
7	0.05	12	12	0.058
8	0.15	12	12	0.058
9	0.05	6	6	0.117
10	0.15	6	6	0.117
11	0.05	12	6	0.117
12	0.15	12	6	0.117
13	0.05	6	12	0.117
14	0.15	6	12	0.117
15	0.05	12	12	0.117
16	0.15	12	12	0.117

bounded flows. It shows good results for boundary layer which are subjected to adverse pressure gradients. The model gives good results at low *Re*, however, it requires very fine meshing near the surface. It solves transport equation for kinematic eddy viscosity without calculating the length scale.

Fig. 6. Comparison of different turbulence models.

For validation purposes, the experimental results of the baseline geometry are compared with the computational model. The computational model of the fan is created in Gambit® and then simulated in Fluent®. Computational and experimental results are compared and error is less than 5%. From, Fig. 6 the velocity magnitude is maximum at the centre of the blade and decreases as we move towards the tip due to tip pressure leakage.

2.6. Generation of Design Space

In this study, a total of four design variables are selected for study. These variables are forward sweep, root angle of attack, tip angle of attack and tip width. Each variable has two levels, high and low. The selection of bounds is based on packaging and fabrication constraints.

The range of four design variables and response parameters are shown in Table 2.

Volumetric flow rate is measured in the form of air delivery. It is defined as volumetric rate of change of air per unit time. Velocity is measured 1.5 m below the ceiling fan for both cases computationally and experimentally. Torque is the tendency of a force to rotate an object about an axis. Energy efficiency is ratio of volumetric flow rate to torque and its unit is $m^2 / min.N$.

After identifying the parameters, levels and response variables, full factorial Design of Experiment (DOE) is applied. There are total four variables and each factor associated with two levels makes $2^4 = 16$
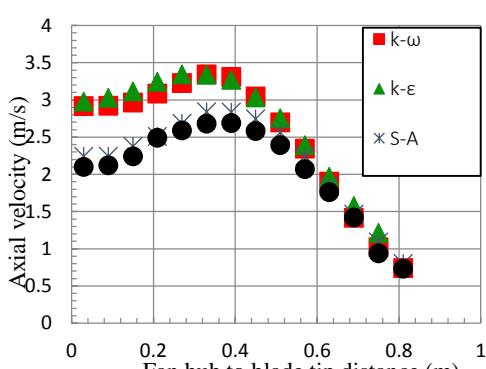
Table 4 Contrast table and value of volumetric flow rate, torque & energy efficiency

Runs	Geometric Parameters				Interactions of Geometric Parameters											Results		
	A	B	C	D	AB	AC	AD	BC	BD	CD	ABC	ABD	ACD	BCD	ABCD	Volumetric Flow Rate (m³/min)	Torque (N.m)	Energy Efficiency (m²/N.min)
1	-	-	-	-	+	+	+	+	+	+	-	-	-	-	+	97.9	0.56	174.7
2	+	-	-	-	-	-	-	+	+	+	+	+	+	-	-	102.3	0.61	166.6
3	-	+	-	-	-	+	+	-	-	+	+	+	-	+	-	125.3	0.78	158.9
4	+	+	-	-	+	-	-	-	-	+	-	-	+	+	+	129.4	0.86	149.5
5	-	-	+	-	+	-	+	-	+	-	+	-	+	+	-	116.8	1.02	113.9
6	+	-	+	-	-	+	-	-	+	-	-	+	-	+	+	133.7	1.09	121.6
7	-	+	+	-	-	-	+	+	-	-	-	+	+	-	+	170.3	1.43	118.3
8	+	+	+	-	+	+	-	+	-	-	+	-	-	-	-	174	1.66	104.2
9	-	-	-	+	+	+	-	+	-	-	-	+	+	+	-	101.6	0.62	162.9
10	+	-	-	+	-	-	+	+	-	-	+	-	-	+	+	105.9	0.68	114.6
11	-	+	-	+	-	+	-	-	+	-	+	-	+	-	+	128.6	0.86	149.4
12	+	+	-	+	+	-	+	-	+	-	-	+	-	-	-	130.8	0.9	144.3
13	-	-	+	+	+	-	-	-	-	+	+	+	-	-	+	133	1.15	115.4
14	+	-	+	+	-	+	+	-	-	+	-	-	+	-	-	138.3	1.34	102.9
15	-	+	+	+	-	-	-	+	+	+	-	-	-	+	-	170.6	1.59	106.7
16	+	+	+	+	+	+	+	+	+	+	+	+	+	+	+	185.3	1.76	104.8

experiments through full factorial design model. These blades are computationally designed with a combination of these parameters. The 16 combinations of design variables with different levels result in the development of design matrix as represented in Table 3.

3. RESULT AND DISCUSSION

3.1. Parametric Studies

The velocity profiles of all designed experiments are shown in Fig. 7 and Fig. 8. A consistent behaviour is detected for all blades that the velocity is higher around 0.3-0.4 m and significantly decreases towards the blade tip. The velocity near the blade tip is less due to formation of tip vortices. The maximum velocity is achieved near hub and starts decreasing gradually and shows minimum values near the blade tip.
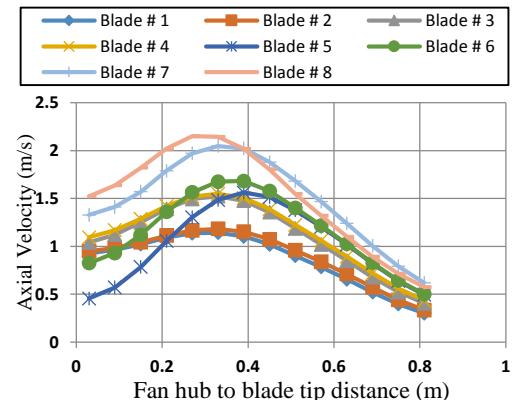

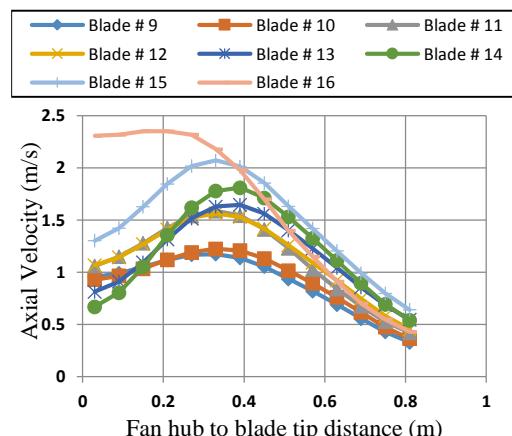**Fig. 7. Velocity profile for 3 blade ceiling fan (1-8).**

Fig. 8. Velocity profile for 3 blade ceiling fan (9-16).

Blade number 16 shows the maximum velocity below 1.5 m of the ceiling fan. It should be noted that the values of the geometric parameters are all set high for blade number sixteen.

Pressure and velocity contours of blade number 1, 2, 8, 12 and 16 are shown in Fig. 9 and Fig. 10. Pressure contours show that large region of low pressure is created on upper side of ceiling fan blades with a high forward sweep.

The two levels considered for forward sweep are 0.05 and 0.15 m. Blade designs 1, 3, 5, 7, 9, 11, 13 and 15 are compared with 2, 4, 6, 8, 10, 12, 14 and 16 respectively that have a high sweep angle. It is observed that forward sweep has moderate effects on the volumetric flow rate as shown in Table 4. By increasing forward sweep, the area of leading edge is increased that comes in contact with the fluid first.
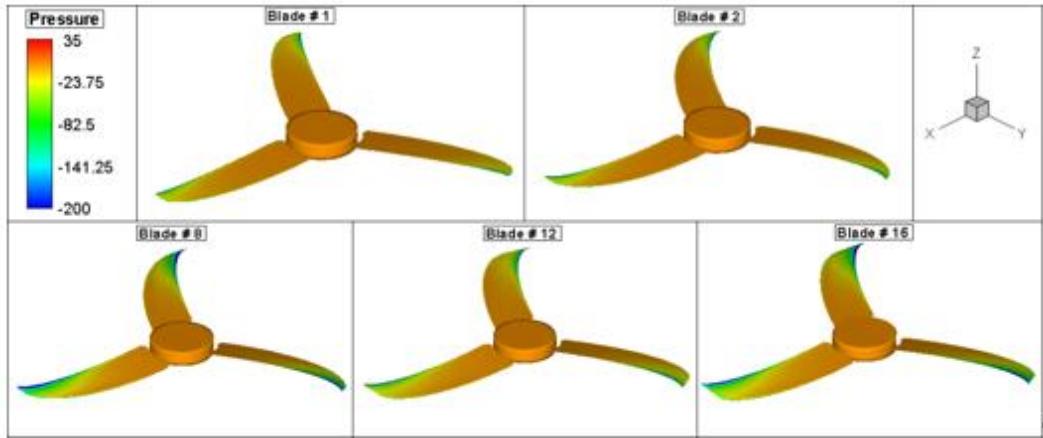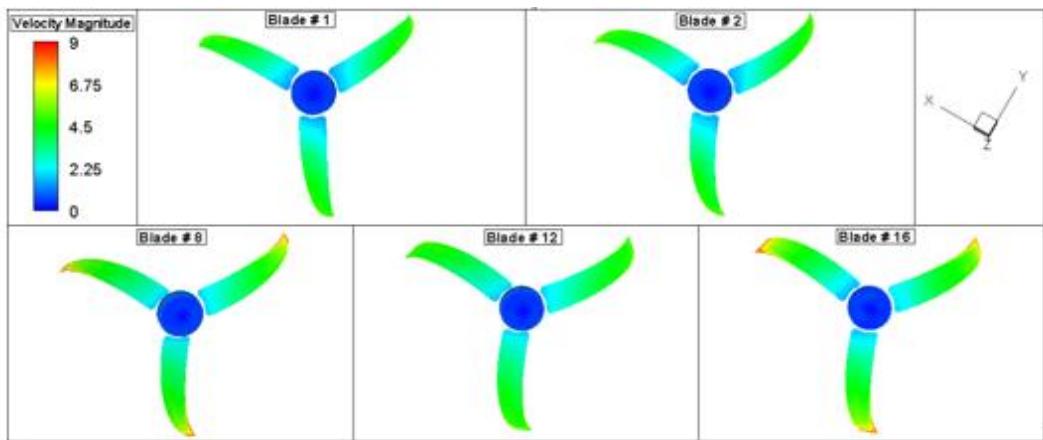
Fig. 9. Pressure contours of fan blades.

Fig 10. Velocity contours of fan blades

This redirects more volume of the fluid downwards. Similarly, the values of torque and energy efficiency are also shown in Table 4.

3.2. Sensitivity Analysis

Effect on Volumetric Flow Rate

After getting the results, the sensitivity analysis of variables and associated interactions are calculated using Minitab ®.

From perspective of comparison, sign of effects is not significant but it is the magnitude which governs the response of the system. Table 4 shows contrast table & value of volumetric flow rate, torque & energy efficiency for all 16 blades.

$$Effect\ of\ Parameter = \frac{Contrast}{n2^{k-1}} \qquad (11)$$

where *n* is replication of results, (with *n=1* and *K-1=3*). Effect of geometric parameter and interactions are calculated for volumetric flow rate, torque and energy efficiency as shown in Fig. 9.

The results indicate that parameter C (Tip angle of attack) and B (Root angle of attack) are most sensitive for volumetric flow rate. The interaction BC (Tip and Root angle of attack), Parameter A (forward swept) and D (Tip width) have a medium effect on the volumetric flow rate (Fig. 9). All other

parameters and their interactions are less sensitive and have a small effect on the volumetric flow rate. This concludes that tip angle of attack and root angle of attack are more important or sensitive for volumetric flow rate while as opposed to forward sweep and tip width and their interactions. The findings are consistent with the conventional wing theory. Contour plots which elaborate the effect of geometric parameters on volumetric flow rate are shown in Fig 12. The contour graph show relationships between two variables on volumetric flow rate. The other two parameters are kept in their middle settings like geometric parameter A is held at 0.10 m while its low setting is 0.05 m and high setting is 0.15 m. From these graphs high regions of volumetric flow rate confirm that parameter C is most important. The increase in volumetric flow rate is recorded with the increase in value of B and C. A similar trend is found between A and C. Simultaneous increase in A and C result the volumetric flow rate to increase although it is less in magnitude compared to B and C. Commenting on other relations, it can be said that when D is in relation to B and C, an increase in the value of B and C, helps to increase the volumetric flow rate. So, it can be concluded that air delivery follows the increasing trend when parameters A, B and C moves from lower value towards higher value.
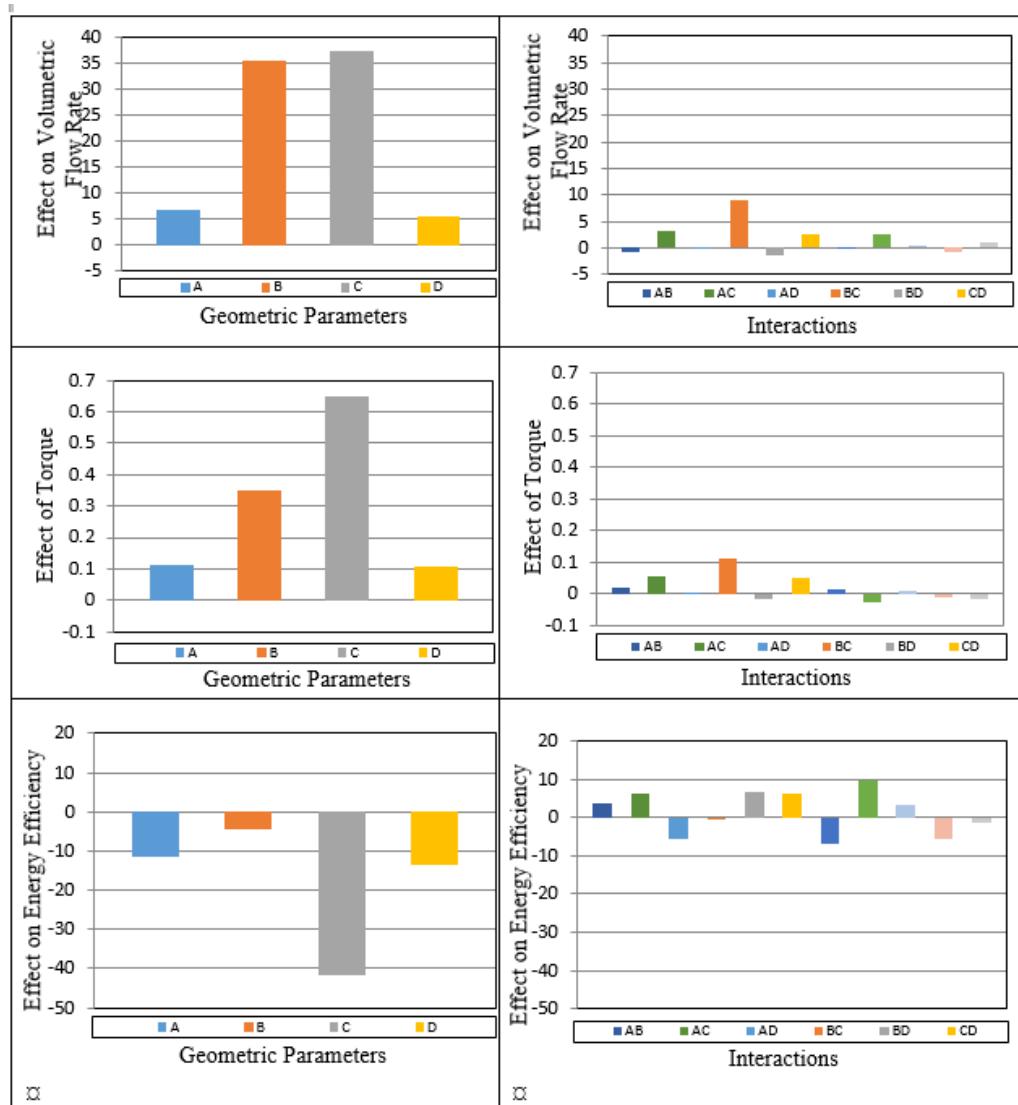
Fig. 11. Effect of parameters and interaction on volumetric flow rate, torque and energy efficiency.
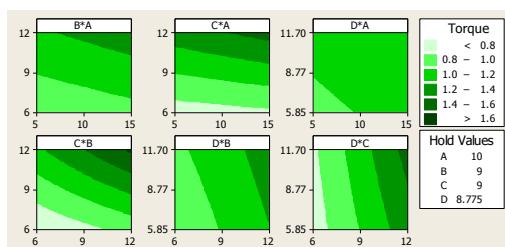

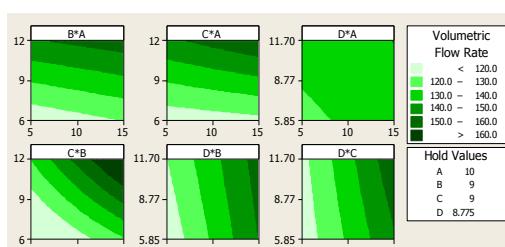**Fig. 12. Changing parameters and volumetric flow rate.**

Fig. 13. Changing parameters and torque.

Table 5 Constraints on Multi-optimization for 3 blades ceiling fan

Constraints and their range for optimization
$130 \leq V$
$T \geq 1.3$
$140 \leq E_f$

Effect on Torque

From effect of all variables, the most sensitive geometric parameter for torque is C (Tip angle of attack), B (Root angle of attack), A (Forward sweep), D (Tip width) and BC (Root and Tip angle of attack) shown in Fig. 9. All other parameters are with less magnitude and less sensitive for torque in comparison to the above parameters and interaction. Relationship between two variables on torque is shown in Fig 13 while the other two parameters are kept in their middle settings.

Contours are plotted to capture effect of variation in

geometric parameters on torque. The light region in the graph shows less torque and dark region shows higher magnitude of torque. Fig 13 shows graphs between parameter C and D, as both parameters setting increased from the lower limit to upper limit the torque of the ceiling fan blade is increased. By neglecting all other parameters and considering only torque factors, then parameters B, C and D should be moved from higher to lower boundary limits and parameter A from higher to lower boundary limit.

Effect on Energy Efficiency

Energy efficiency is the ratio of volumetric flow rate to torque. As shown in Fig. 9, parameter C (tip angle of attack) has a maximum magnitude followed by D (tip width), A (forward sweep) and ABD (forward sweep, root angle of attack and tip width). Remaining all other geometric parameters and interactions are less significant for energy efficiency due to their smaller values.

Relationship between two variables on energy efficiency is shown in Fig 14 while other two parameters are kept in their middle settings. The dark regions in the graph represent high value of energy efficiency and light value represents low value of energy efficiency. The reduction in values of parameter A and C increase energy efficiency. It is established that the energy efficiency increases as parameters A, B, C and D move from higher values toward lower boundary limit.
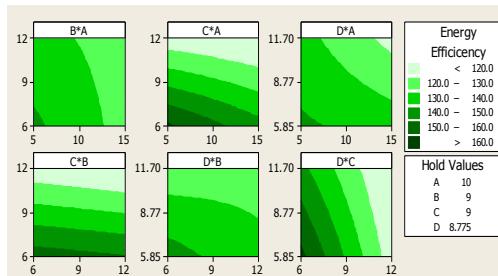

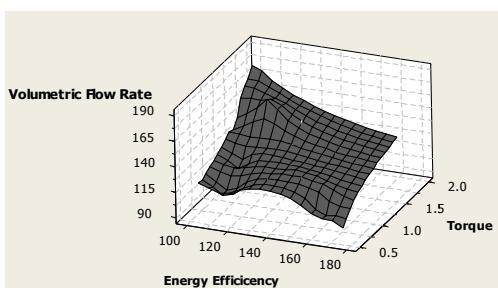**Fig. 14. Changing parameters and energy efficiency trends.**

Fig. 15. Response surface for 3 blade ceiling fan.

3.3. Multi Objective Optimization

For performance optimization, a statistical analysis technique, Response Surface Method (RSM), is used which shows the relationship between different variables and responses. All three performance indicators are considered collectively and multi-objective optimization approach is adopted. The

expected results of optimum solution showed improvement for all 3-responses. The design space is shown in Fig 15. The control variables used for optimization are

$$J = [V, T, E_f] \tag{12}$$

The objective function for optimization is

$$J = -w_1 V + w_2 T - w_3 E_f \tag{13}$$

The first term of objective function in Eq. (13) represents the volumetric flow rate, second term represent torque and the last term represents the energy efficiency of the ceiling fan. In this study the weighting factors used are $w_1 = w_2 = w_3 = 1$. The main purpose of the objective function is to increase the volumetric flow rate for a ceiling fan, decrease its torque and increase the energy efficiency of the ceiling fan. The constraints applied on the search space are shown in Table 5.

Figure 16. shows all 3-responses at the optimum setting of geometric parameters which is represented by red line showing the current settings. All responses carried its own desirability and the composite desirability is 0.84484 which shows that the final design is very reliable for all performance indicators. The horizontal blue dotted lines are showing the level of response at these settings of parameters. For verification, this final design is computationally made in Gambit® and simulated in Fluent®. High degree of confidence is demonstrated between predicted values and reported readings.
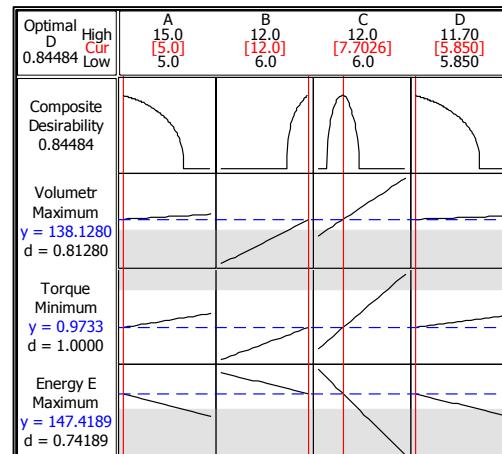

Fig. 16. Multi-Objective optimum solution for 3 blade ceiling fan.

4. CONCLUSION

In this work, parametric study is carried out to find the effect of parameters on the ceiling fan. The data of air velocity for the benchmark design are collected experimentally. Using DOE, sixteen different experiments are designed based on four variables through full factorial approach. Reynolds Averaged Navier Stokes approach is used to simulate the designs. After a sensitivity analysis, the root and tip angle of attack are found to be more sensitive for

volumetric flow rate, torque and energy efficiency. Forward swept parameter showed a moderate effect on response parameters. Tip width is the last parameter that showed the minimum effect on all response parameters. Design number sixteen showed the maximum air flow rate and associated set of all four parameters were set to high. Using RSM an optimized design is proposed in which volumetric flow rate is increased, torque reduced, and energy efficiency of ceiling fan increased.

ACKNOWLEDGEMENT

REFERENCES

Adeeb, E., A. Maqsood and A. Mushtaq (2015). Effect of Number of Blades on Performance of Ceiling Fans. *4th International Conference on Advances in Mechanics Engineering*, Spain, MATEC Web of Conferences.

Adeeb, E., A. Maqsood, A. Mushtaq and Z. Hussain (2015). Shape Optimization of non-linear swept ceiling fan blades through RANS simulations and Response Surface Methods. *12th International Bhurban Conference on Applied Sciences and Technology*, IEEE.

Afaq, M. A., A. Maqsood, K. Parvez and A. Mushtaq (2014). Study on the design improvement of an indoor ceiling fan. *11th International Bhurban Conference on Applied Sciences and Technology*, IEEE.

Amano, R. S., E. K. Lee, C. Xu and J. Xie (2005). Investigation of the Unsteady Flow Generated by an Axial Fan: Experimental Testing and Simulations. *International Journal of Rotating Machinery* 3, 256-263.

Ankur, J., R. U. Rochan, C. Samarth, S. Manish and K. Sunil (2004). Experimental Investigation of the Flow Field of a Ceiling Fan. *ASME 2004 Heat Transfer/Fluid Engineering Summer Conference*, Charlotte, North Carolinia, USA.

Azim, M. A. (2014). Velocity field analysis of a ceiling fan. *Turkish Journal of Engineering, Science and Technology* 01, 1-7.

Aziz, M. A., I. A. M. G. Shahat, F. A. Mohammed and R. H. Mohammed (2012). Experimental and numerical study of influence of air ceiling diffusers on room air flow characteristics. *Energy and Buildings* 55, 738–746.

Bhortake, R. V., P. S. Lachure, S. R. Godase, V. V. More and K. S. Chopade (2014). "Experimental Analysis of Air Delivery in Ceiling Fan."

International Journal of Emerging Technology and Advanced Engineering 4(6), 247-251.

Chiang, H. C., C. S. Pan, H. S. Wu and B. C. Yang (2007). Measurement of Flow Characteristics of a Ceiling Fan with Varying Rotational Speed. In *Proceedings of Clima 2007 WellBeing Indoors.*

Falahat, A. (2011). "Numerical and Experimental Optimization of Flow Coefficient in Tubeaxial Fan." *International Journal of Multidisciplinary Sciences and Engineering* 2(5), 24-29.

Ho, S. H., L. Rosario and M. M. Rahman (2005, August). Effect of using ceiling fan on human thermal comfort in Air-conditioned space. In Procedings of 3rd International Energy Conversation Engineering Conference, San Francisco, California

Idahosa, U., V. V. Golubev and V. O. Balabanov (2008). " An automated optimal design of a fan blade using an integrated CFD/MDO computer environment." *Engineering applications of computational fluid mechanics 2(2), 141-154*

Jafari, M., H. Afshin, B. Fahanieh and H. Bozorgasareh (2015). Numerical Aerodynamic Evaluation and Noise Investigation of a Bladeless Fan. *Journal of Applied Fluid Mechanics* 8(1), 133-142.

Lin, S. C. and M. Y. Hsieh (2014). An Integrated Numerical and Experimental Analysis for Enhancing the Performance of the Hidden Ceiling Fan. Hindawi.

Lin, S. C., M. Y. Hsieh and C. J. Chang (2013). Performance Improvement of a Hidden Ceiling Fan. *Applied Mechanics and Materials* 479 - 480, 279-283.

Lubliner, M., J. Douglass, D. Parker and D. P. Chaser (2004). Performance and applications of gossamer wind solar powered ceiling fans. In Procedings of 25th AIVC Conference "Ventilation and Retrofitting", Prague, Czech Republic.

Maqsood, A., J. Masud and A. Mehdi (2007). Aerodynamic Evaluation of Wing-Strake Modification by Higher Order Panel Method. *45th AIAA Aerospace Science Meeting and Exhibit*, Nevada, USA, American Institute of Aeronautics and Astronautics.

Momoi, Y., K. Sagara, T. Yamanaka and H. Kotani (2004). Modeling of ceiling fan based on velocity measurement for CFD simulation of airflow in large room. In *Proceedings of 9th international conference on air distribution in rooms,* Coimbra, Portugal.

Nawaz, B. A., B. M. Kanti and C. Abhijit (2012). An Intelligent Approach of Regulating ElectricFan Adapting to Temperature and Relative Humidity. *MECS* 61-69.

Parker, D. S., M. P. Challahan, J. K. Sonne, G. H. Su and B. D. Hibbs (2000). *Development of a High*

Efficiency Ceiling Fan. Improving Building Systems in Hot and Humid Climates, Texas A&M University.

Prabhakaran, S. and M. S. Kumar (2012). Development of Glass Fiber Reinforced Polymer Composite Ceiling Fan Blade. *International Journal of Engineering Research and Development* 2(3), 59-64.

Ramadan, B. and S. K. Nadar (2011). "Studying the Features of Air Flow Induced by a Room Ceiling-Fan." *Energy and Buildings* 43(8), 1913-1918.

Rizk, A., A. El-Deberky and N. Guirguis, M (2015). Simulation Comparison Between Natural and Hybrid Ventilation by Fans at Nighttime for Severe Hot Climate (Aswan, Egypt). Renewable Energy in the Service of Mankind 1(1) 609-620

Sathaye, N., A. Phadke, N. Shah and V. Letschert (2012). Potential Global Benefits of Improved Ceiling Fan Energy Efficiency. LBNL Report Ernest Orlando Lawrence Berkeley National Laboratory, United States

Schiavon, S. and A. K. Melikov (2008). Energy saving and improved comfort by increased air movement. *Energy and Buildings* 40(10), 1954-1960.

Schmdit, K. and D. J. Patterson (2001). Performance result for a high efficiency tropical ceiling fan and comparisons with conventional fansdemand side management via small appliance efficiency. *Renewable energy* 22(3), 169-176.

Singh, O. P., M. Garg, V. Kumar and Y. V. Chaudhary (2013). Effect of Cooling System Design on Engine Oil Temperature. *Journal of Applied Fluid Mechanics* 6(1), 61-71.

Sivakumar, V. M., A. Surendhar and T. Kannadasan (2015). Prediction of Air Flow and Temperature Distribution Inside a Yogurt Cooling Room Using Computational Fluid Dynamics. *Journal of Applied Fluid Mechanics* 8(2), 197-206.

Spalart, P. R. a. A., S. R. (1992). A One-Equation Turbulence Model for Aerodynamic Flows. in Proceddings of Aerospace Sciences Meeting and

Tripathi, B. and S. G. Moulic (2012). Investigation of Air Drafting Pattern Obtained from the Variation in Outlet Positions inside a Closed Area. *Journal of Applied Fluid Mechanics* 5(4), 1-12.